Analysis of Solar Irradiance Variation on Heat Flux and Temperature Distribution for a Dish Concentrator Receiver

Endeshaw Alemu Bekele[1]
Faculty of Mechanical Engineering;
Jimma Institute of Technology,
Jimma University,
P.O. Box 378, Jimma, Ethiopia
e-mail: alemu.endeshaw@ju.edu.et

Venkata Ramayya Ancha
Faculty of Mechanical Engineering;
Jimma Institute of Technology,
Jimma University,
P.O. Box 378, Jimma, Ethiopia
e-mail: dra.venkata@ju.edu.et

Tarekegn Limore Binchebo
Faculty of Mechanical Engineering;
Jimma Institute of Technology,
Jimma University,
P.O. Box 378, Jimma, Ethiopia
e-mail: tarekegn.limore@ju.edu.et

Concentrated solar power presents immense scope for the deployment of small-scale units focusing on diverse applications, including process heat and rural on/off-grid applications. This paper presents the analysis of solar irradiance variation on heat flux and temperature distribution at the dish concentrator receiver. A solar dish concentrator with a 2.8-m aperture diameter and a 0.4-m depth was used for this analysis. The solar ray intersection between a dish concentrator and its receiver, along with the heat flux distribution prediction, was carried out using SolTrace. The effect of flux intensity variation on temperature distribution at the receiver was investigated using COMSOL MULTIPHYSICS. The optical analysis considered 10,000 rays, and 91.65% of them were observed to reach the surface of the receiver. For 1000 W/m^2 of beam solar radiation, a peak heat flux and maximum temperature at the concentrator's focal plane are found to be 32.4 MW/m^2 and 923 K, respectively. The validation had been done using previously reported results in the literature to verify the correctness of the present simulation results. The effect of beam solar radiation variation on heat flux intensity and the temperature distribution revealed that both heat flux and temperature increase with increasing solar radiation, which points out the influence of design and operating conditions. Apart from PillBox and Gaussian distributions, the effect of slope and specularity errors was characterized, suggesting a greater sensitivity to the former than the latter. [DOI: 10.1115/1.4053963]

Keywords: dish concentrator, heat flux, receiver, SolTrace, temperature distribution

1 Introduction

The impact of climate change and the increasingly diminishing supply of fossil fuels necessitates the utilization of renewable energy across the world. Solar energy is a highly preferred alternative energy source because it is affordable and environmentally friendly. Concentrated solar power (CSP) that enables the attainment of higher and higher temperatures is utilized for power generation, irrigation, cooking, water heating, desalination, and water distillation applications [1].

The solar radiation that ultimately (not all) reaches the receiver absorbing surface will be transferred to a working fluid retained inside the concentrator's receiver to produce the desired thermal energy output. The concentration ratio is the ratio of aperture area to receiver area, which determines the heat flux on the receiver surface and the resultant temperature attained by the working fluid inside. The amount of thermal energy transferred to the working fluid and the system's overall efficiency is greatly dependent on the surface heat flux and its variation, which by itself has implications for material selection and structural integrity. Realizing this, numerical and experimental investigations have been carried out in the past to characterize the heat flux distribution on the CSP absorber/receiver.

A numerical simulation of flux intensity distribution at the absorber of various types of the concentrator, such as parabolic dish, parabolic trough, and solar heliostat, was performed using a Monte Carlo ray tracing (MCRT) method. The solar flux distribution on the receiver of a parabolic dish concentrator system was studied by Qianjun et al. [2]. They use the MCRT method to analyze the influence of incident solar radiation, aspect ratio, and system error. Both aspect ratio and system error have been shown to influence flux distribution substantially. Senthil and Cheralathan [3] experimentally investigated the effect of receiver surface temperature distribution on heat gain and losses of parabolic dish concentrators. The heat loss increased at the region closer to the periphery of the receiver due to higher surface area and compounded by a higher temperature. The surface temperature of a dish concentrator receiver was observed to increase with beam solar radiation and decrease with wind speed. Further, they also explored two-fluid flow directions (straight and curved path) to identify the effective heat absorption and reduce the operational duration. Compared to a straight path, fluid flow in a curved channel improved thermal efficiency by 3.8% and reduced operation time by 20%.

A three-dimensional (3D) ray-tracing model was proposed by Nyeinga et al. [4] for evaluating solar flux distribution of a small-scale solar dish concentrator for cooking purposes. They developed an algorithm for ray-tracing using Matlab and analyzed flux distribution for a continuous reflecting surface and flat mirror-tiled surface. For a continuous reflecting surface, a ray gets concentrated on a small area with high flux intensity, while a reflector with mirror tiles, an enlarged image centered on the focal point, was formed with low flux intensity. Zhang et al. [5] conducted a comprehensive study on the effects of truncation positions of a new type of truncated compound parabolic concentrator (CPC) to investigate the optical performance, temperature distribution of PV, energy, and exergy efficiencies of concentrating photovoltaic and thermal systems. Based on direct absorption collection, Zhang et al. [6] presented a novel spectral splitting concentrating photovoltaic/thermal prototype. The concentrator is a truncated CPC by eliminating solar radiation's multiple reflections (EMR). The radiation transfer model was established based on the incidence angle distribution of the

[1]Corresponding author.

Manuscript received November 4, 2021; final manuscript received February 24, 2022; published online March 10, 2022. Assoc. Editor: Guihua Tang.

solar irradiance illuminating on the filter at the outlet aperture of the EMR concentrator.

Using Tracepro software, Pavlovic et al. [7] examined an optical design of a parabolic solar concentrator with a diameter of 3800 mm and 12 curvilinear trapezoidal reflecting facets. They presented an optical simulation of heat transfer on the solar cavity receiver-spiral corrugated pipe and irradiance distribution for absorbed energy at the center and peripheral receivers. Zhang et al. [8] investigated the optical performance and multi-objective optimization of GaAs solar cells to improve the photo-electronic capacity. Nie et al. [9] proposed a concave quartz window to enhance the flux uniformity of the cylindrical cavity receiver of the solar dish concentrator. Four types of concave quartz windows, including conical, spherical, sinusoidal, and hyperbolic tangents, were employed for the analysis. Fontani et al. [10] performed the optical ray-tracing analysis to predict the shape of the light spot on the receiver of a Scheffler-type concentrator. Santos et al. [11] also developed an analytical method to compute the optical analysis of linear Fresnel reflection with a flat receiver. Ciscenor-Cardenas et al. [12] reported a theoretical and experimental study of the radiation flux distribution in a parabolic dish concentrator to determine the homogeneous irradiance distribution and global error. Jian et al. [13] investigated the influence of dish concentrator geometry factors on the optical performance of cavity receivers. The analysis is carried out through OptisWorks ray-tracing software, which shows that the optical performance increases as the rim angle decreases while the uniformity of radiative heat distribution on the absorber decreases. Using selective conical-shaped mechanical protrusions inside the irradiated cavity surface, Bopche et al. [14] improved the performance of a modified cavity receiver of a parabolic dish concentrator. Their study intends to increase the amount of irradiated concentrated solar energy while reducing system losses. The finding shows that a dish concentrator's thermal efficiency improved by about 1.23–1.31% on average. Lee et al. [15] analyzed wavelength-selective solar- thermal absorber with two-dimensional nickel gratings, a thin SiO_2 film, and Nickel substrate for high-temperature applications. To improve the solar-thermal conversion efficiency, Yang et al. [16] proposed a selective solar absorber based on nano-multilayered AlCrSiO films synthesized by a cathode arc ion plating method. They examined the absorber's thermal stability at 600 °C and 700 °C. The absorber reached thermal equilibrium with a selectivity of 0.923 absorbances and 0.161 emittances in the air for 200 h. Zhang et al. [17] used a Multi-Island Genetic Algorithm (MIGA) to optimize the arrangement of selective solar absorbers. The selective solar absorber is equipped with the set of optimal geometric parameters that exhibits the solar absorptance greater than 0.932 with a probability of 96% and mid-infrared emittance lower than 0.053 at the same time.

Aggrey et al. [18] numerically investigated a parabolic trough receiver tube's heat flux and temperature distribution. The heat flux was estimated through Monte Carlo ray tracing and coupled with computational fluid dynamics (CFD) for heat transfer analysis in the receiver. In particular, they examine the effect of rim angle, concentration ratio, fluid temperature, and Reynolds number on temperature distribution at an absorber tube.

Zhao et al. [19] also performed a simulation of heat flux distribution on an absorber surface of parabolic trough collector (PTC) considering the effect of non-parallelism of solar rays with cone optics, geometric concentrating ratio, rim angle, the transmittance of the glass tube, the reflectivity of the glass tube, absorption of the absorber tube, and reflectivity of the parabolic trough mirror. Furthermore, a numerical investigation on the impact of slope errors and specularity errors on the thermal performance of a solar parabolic trough collector system was studied by Aggrey et al. [20]. Wang et al. [21] conducted a review on sun shape ad slope error modeling approaches in MCRT for concentrated solar power systems. They used six optical modeling tools, including Tonatiuh, SolTrace, Tracer, Solstice, Heliosim, and Solarpilot, to develop a sun shape and surface slope error model.

Butti et al. [22] modeled a 5.8-kW solar biomass gasification reactor coupled to the cylindrical cavity receiver of a parabolic dish concentrator. They used the Monte Carlo ray tracing method and computational fluid dynamics to generate a heat flux map and temperature field on the surface of the cavity receiver. Yan et al. [23] developed two-mirror rearrangement strategies and their optimization approach by utilizing a novel ray-tracing method and a genetic algorithm to investigate uniform flux distribution on the absorber surface inside the cavity of a dish concentrator. The two mirror configurations (mirror rotation and mirror translation) improve flux distribution homogeneity, optical efficiency, and direct useful energy ratio. The suggested Motion Accumulation Ray-Tracing (MART) optimization approach enhances the computation efficiency of the flux distribution on the cavity receiver while reducing computational time. Kopalakrishnaswami and Natarajan [24] proposed a numerical analysis of a modified conical cavity receiver to compare its efficiency with other existing solar dish concentrator receivers. They performed a ray-tracing analysis using COMSOL MULTIPHYSICS to determine the size of the receiver, and the result depicts that the proposed receiver has minimum losses and better performance.

Qianjun et al. [25] investigated radiation flux in the focal plane of the dish concentrator receiver employing three different focal lengths. The radiation flux distribution was ascertained using Monte Carlo ray tracing for the frustum, inverted frustum, cylindrical, and conical receiver types. The result depicts that the heat flux distribution of the cylindrical receiver has the best performance among all four receivers, which will result in higher efficiency of the system. Evangelos et al. [26] numerically examined and optimized the optical and thermal performance of cylindrical, rectangular, spherical, conical, and cylindrical–conical cavity receivers for a dish concentrator. The result shows that the cylindrical–conical cavity receiver has the best heat flux and fluid temperature distribution with improved thermal efficiency.

In designing and analyzing the performance of the solar-thermal receiver, the solar heat flux intensity and temperature distribution on the receiver will be the significant parameters. These parameters can be calculated by considering the optical performance of the concentrator with ray-tracing software or using the Monte Carlo ray tracing method. The previous literature described the method of determining heat flux and temperature distribution on several dish concentrator receivers. Most of the works focused on predicting heat flux and temperature distribution using ray-tracing and computational software. However, solar irradiance variation on heat flux intensity and the resultant temperature distribution has not been studied. In this regard, the focus of this work comprises an investigation of the variation of direct normal irradiance on both heat flux and temperature distributions. The heat flux distribution was computed through SolTrace ray-tracing software while considering the effect of slope and specularity errors. The effect of heat flux intensity on temperature distribution was estimated through COMSOL MULTIPHYSICS to determine the peak temperature at the focal plane of the dish concentrator. An investigation of beam solar radiation variation on both heat flux and temperature distribution at the concentrator's focal plane was also carried out in this work.

2 Modeling of Dish Concentrator

A parabolic dish is a two-axis tracking collector that concentrates solar energy into a receiver situated at the dish's focal point [27]. The incoming solar radiation focused on the single focal point, i.e., all sun rays are parallel to the parabola axis directed toward the receiver, as shown in Fig. 1. Based on their structure, solar dish concentrators can be classified as single dish and multi-dish concentrators [28]. It consists of a parabolic-shaped mirror, receiver, support, and tracking system. The dish is mounted on a structure that continuously supports and tracks the sunlight throughout the day. Support structure anchors the entire system to the ground. The tracking system of the dish concentrator consists of a bi-axial tracking device that makes a dish timely follow the movement of the sun in the sky [29]. The tracking device allows the

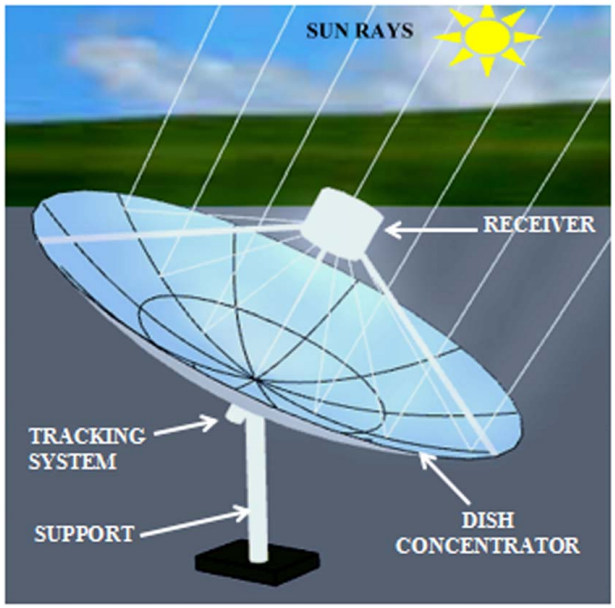

Fig. 1 Overview of a dish concentrator

parabolic-shaped mirrors to maximize the amount of solar energy reflected onto the absorber and achieve a useful high heat and high working fluid temperatures [30]. A receiver is located at the focal point of the dish concentrator to convert the concentrated solar radiation into thermal energy through a heat transfer fluid kept inside it.

The shape of the solar parabolic dish is obtained through the x and y coordinates for a selected point using 3D modeling software. Each coordinate point of the parabola is calculated using Parabola Calculator software. The calculated values are obtained for 16 points in the parabolic curve.

A mathematical equation of parabolic dish concentrator in a Cartesian coordinate system is defined as follows:

$$x^2 + y^2 = 4fz \tag{1}$$

where x and y are coordinates in the aperture plane, z is the distance between the vertex and the paraboloid axis of symmetry, measured along a line parallel to it, and f is the focal length of the parabola.

The Equation of parabola that represents the coordinate of this parabolic curve is given as

$$y = ax^2 + bx + c$$

where a, b, and c are constant with, $a = 2.788 \times 10^{-4}$, $b = 0$, and $c = 3.638 \times 10^{-16}$ values. By substituting the values into the Equation, the Equation of the parabola could be as follows:

$$y = 2.788 \times 10^{-4}x^2 + 3.638 \times 10^{-16}$$

The x and y coordinates of the modeled dish concentrator obtained through Parabola Calculator 2.0 software are shown in Table 1.

The solar dish concentrator comprises the reflecting material that reflects the radiation falling in the concentrator to the focal point. As illustrated in Fig. 2, the focal length is the distance between the parabola's vertices and the focal point. It is related to the aperture diameter and the depth of the parabola [31]. Focal length can be obtained using Eq. (2)

$$f = \frac{D_c^2}{16 \times h} \tag{2}$$

where f is a focal length, D_c is the diameter of the dish concentrator, and h is the depth.

Table 1 Cartesian coordinates of a modeled parabolic dish

X_1 (m)	Y_1 (m)	X_2 (m)	Y_2 (m)
−1.4	0.4	0.175	0.0625
−1.225	0.306	0.35	0.025
−1.05	0.225	0.525	0.056
−0.875	0.156	0.7	0.1
−0.7	0.1	0.875	0.156
−0.525	0.056	1.05	0.225
−0.35	0.025	1.225	0.306
−0.175	0.0625	1.4	0.4
0	0		

Stine et al.[32] described rim angle as the angle measured at the focus from the axis to the solar parabolic truncated rim. During manufacture, the rim angle impacts the incoming solar radiation and the shape of the parabolic dish [33]. Rim angle varies from less than 10 deg to more than 90 deg [34]. The value of rim angles decreases when the focus point increases [35]. Solar dish concentrators utilize a truncated section of the primary parabolic curve. The rim angle or the ratio of focal length to aperture diameter f/d is commonly used to describe the extent of this truncation [31]. Rim angle is found through Eq. (3)

$$\frac{f}{D_c} = \frac{1}{4\tan\left(\frac{\phi_r}{2}\right)} \tag{3}$$

where f is a focal length, ϕ_r is a rim angle, and D_c is a concentrator diameter.

The receiver collects the energy reflected by the concentrator and transmits it to the working fluid, resulting in usable thermal energy. The absorbing surface is usually placed behind the concentrator's focus to reduce the incident flux intensity [28]. The receiver collects as much reflected solar energy as possible from the dish concentrator. As stated by Hafez et al. [36], the minimum possible diameter of the receiver (D_{rec}) is obtained as follows:

$$D_{rec} = \frac{D_c \times \sin(\theta)}{\sin(\phi_r)} \tag{4}$$

The concentration ratio (C) is the proportion of the aperture area (A_a) to the area of the receiver (A_{rec}). It can be defined as the factor by which the incident energy flux at the aperture area of the concentrator is enhanced optically in the receiving area.

A higher concentration ratio means more heat is transferred to the working fluid and increases its temperature. The receiver's surface heat losses get reduced due to the smaller receiving area, and high energy conversion can be achieved [34]. Concentration ratios vary from unity for flat plate collectors to a maximum of 46,747 for concentrated collectors theoretically [37]. In practice, that limit of solar concentration is unreachable due to non-ideality and losses

$$C = \frac{A_a}{A_{rec}} = \left(\frac{D_c}{D_{rec}}\right)^2 \tag{5}$$

By integrating a differential segment of the primary parabolic curve and applying the constraints $x = h$ and $y = d/2$, arch length (S) may be determined

$$S = \left\{\frac{d}{2}\sqrt{\left(\frac{4h}{d}\right)^2 + 1}\right\} + 2f\ln\left\{\frac{4h}{d}\sqrt{\left(\frac{4h}{d}\right)^2 + 1}\right\} \tag{6}$$

The edge radius (r_r), or maximum distance value between the focus point and the paraboloid extreme, is another important

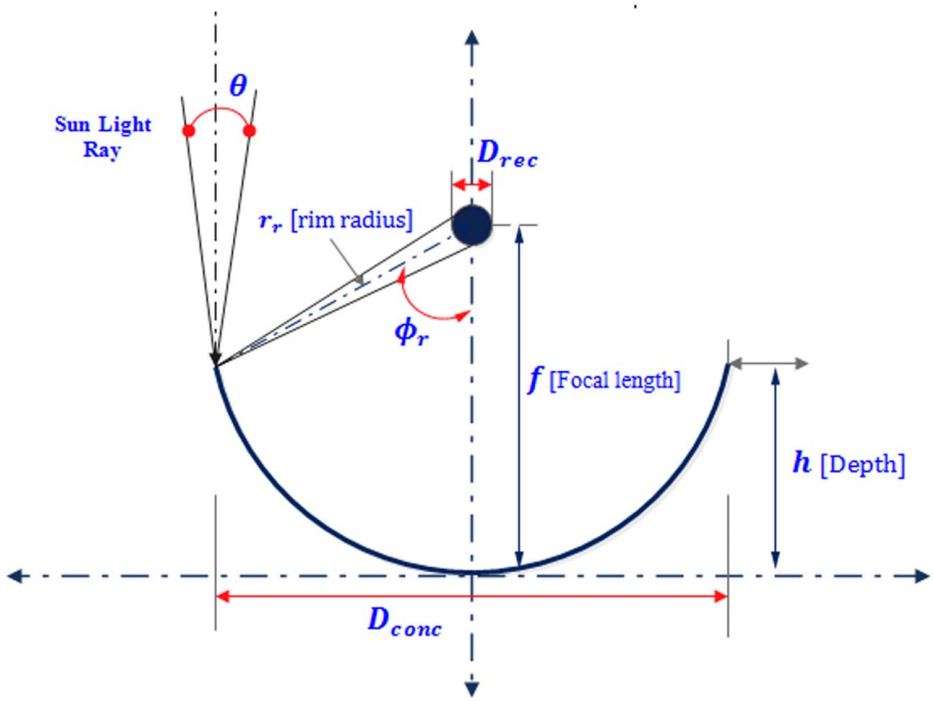

Fig. 2 Schematic diagram of parabolic dish concentrator geometry

Table 2 Design parameter for parabolic dish solar concentrator employed in this study

Parameters	Numerical value	Unit
Aperture diameter	2.8	m
Focal length	1.2	m
Depth of concentrator	0.4	m
Rim angle	59.5	deg
f/d ratio	0.428	–
Minimum possible receiver diameter	0.015	m
Receiver diameter	0.2	m
Arch length	4.067	m
Concentration ratio	196	–
Rim radius	1.625	m

parameter for defining the shape of the solar dish concentrator

$$r_r = \frac{2f}{1+\cos(\phi_r)} \tag{7}$$

Table 2 summarizes the design parameters of the dish concentrator employed in this work. By taking a standard satellite dish having a 2.8-m aperture diameter and a depth of 0.4 m, focal length, rim angle, arch length, receiver diameter, concentration ratio, and rim radius are estimated through Eqs. (1)–(7).

3 Analysis of Concentrated Flux Intensity Using SolTrace Software

SolTrace is an open access ray-tracing software developed by National Renewable Energy Laboratory (NREL). It is used to model and analyze the optical performance of concentrated solar power [38–40]. Furthermore, SolTrace explores the ray intersection and solar flux intensity on the concentrator's receiver [39]. The first step to analyze ray tracing in SolTrace is to define the sun's shape and direction. The sun shape consideration has three options, i.e., Gaussian, PillBox, and user-defined distributions. The non-dimensional azimuthal radiance profile of the direct components of solar irradiance is expressed through sun shape [21]. The next step is setting the optical properties of the concentrator. As shown in Fig. 3, the optical properties include reflectivity, transmissivity, and optical errors. Optical error is defined as the difference between the diameter of the real sun and the diameter of the degraded sun produced by the concentrator mirror [12]. The optical error considered during solar flux distribution analysis is specularity, slope, shape, and tracking system errors. Specularity error is defined relative to the reflected vector [38]. Slope and shape errors occur on account of topographical deviations of the mirror surface. Slope error is related to material production, processing, and finishing of the mirror surface, while shape error refers to the deviation or deformation of a portion of the mirror caused by an external force, like wind or gravity. Tracking errors occur due to an imperfect tracking system [41]. After defining the optical properties, the system geometry was created by setting stage properties and element definitions with those stages. In this work, a two-stage approach was employed for the analysis. The first stage concerns preparing the concentrator geometry, and the last stage refers to the absorber of the concentrator. A stage is a portion of the geometry that is progressively struck by rays propagating from the sun to the focal point of the concentrator's receiver [38].

The input parameter used for analyzing ray tracing using SolTrace is summarized in Table 3. The intended number of ray's intersection and the maximum radiations generated on the concentrator will be set in the ray-tracing option until the simulation converges. A sun rays count of 1,000,000 is required to analyze heat flux distribution, and a 10,000 ray intersection will be needed to estimate the average efficiency of optical receivers. SolTrace generates a ray intersection between the concentrator and its absorber. It also predicts contour and surface plot flux distribution at the concentrator's receiver.

4 Result and Discussion

4.1 Heat Flux Distribution on Focal Plane of the Concentrator. The ray intersection and solar flux distribution at the cylindrical receiver of a concentrator were simulated using the SolTrace software. Figure 4 indicates the ray intersection for a hundred beam solar with the concentrator's absorber/receiver. The

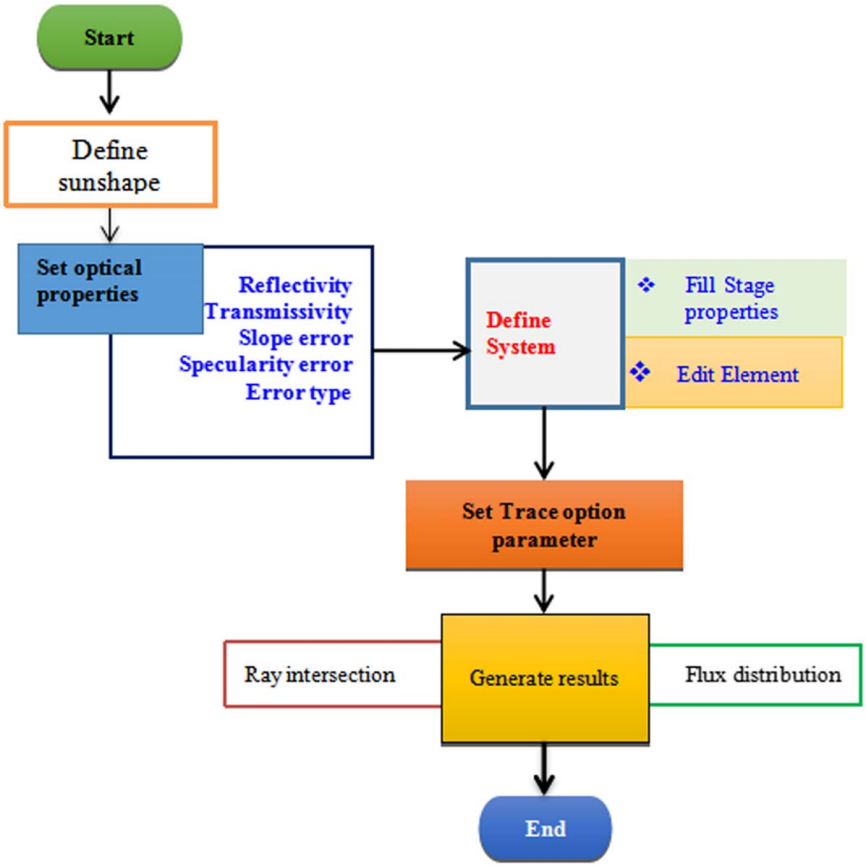

Fig. 3 Flowchart of flux distribution analysis using SolTrace software

Table 3 Input parameter to the SolTrace software

Parameter	Value/type	Unit
Sun shape: Pillbox	4.6	mrad
Sun shape: Gaussian	2.73	mrad
The reflectivity of the concentrator [41]	92	%
Transmissivity [41]	8	%
Slope error [38]	2.5	mrad
Specularity error [38]	0.2	mrad
Error type	Gaussian	–
Desired number of ray intersection	10,000	–
The maximum number of sun rays generated	1,000,000	–

optical analysis was performed for 10,000 rays intersection. Based on simulation results from all emitted rays, 9165 reach the receiver surface or 91.65% of the beam incident. The amount of rays reaching the absorber depends on the concentrator's optical properties like reflectivity and optical errors. The power per ray and total power of the plotted rays was found to be 0.613 W and 5612 W, respectively.

Figure 5 shows the contour and surface plot of the heat flux intensity at the concentrator's focal plane for the direct normal irradiance (DNI) of 1000 W/m^2. The flux profile is generated using SolTrace software at the concentrator's receiver by setting the optical and stage properties.

The peak flux predicted at the receiver is found to be 32.4 MW/m^2 with an uncertainty of +/− 5.76% or 202.4 kW/m^2 deviation. Furthermore, the average heat flux intensity at the concentrator's absorber/receiver reaches around 4.75 MW/m^2. It can be seen that the flux distribution is maximum at the center of the absorber and decreases toward its edge. Since the solar dish concentrator has a

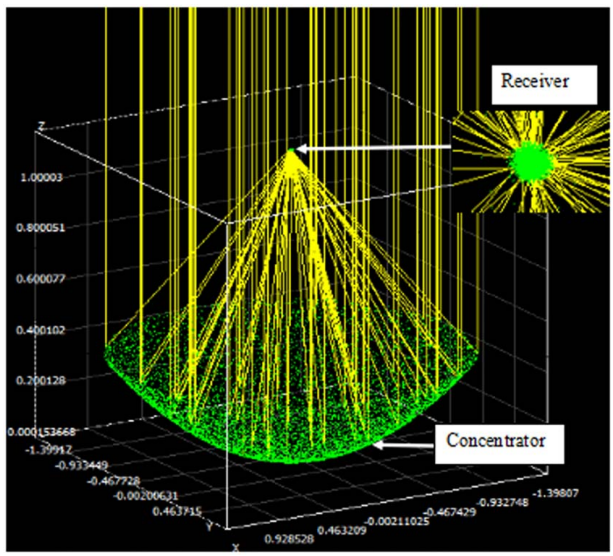

Fig. 4 Ray intersection (scatter) plot on the concentrator and receiver

point focus, the incoming solar radiation concentrated to the focal plane produces peak heat flux at the center of the absorber/receiver. The uniformity of radiation flux at the concentrator receiver varies with the slope and specularity errors. At a low slope error, the flux distribution is relatively uniform; however, as slope error increases, the non-uniformity of the flux reduces peak flux at the center of the receiver. Thus, the optical error could be minimized to enhance the optical efficiency of the concentrator.

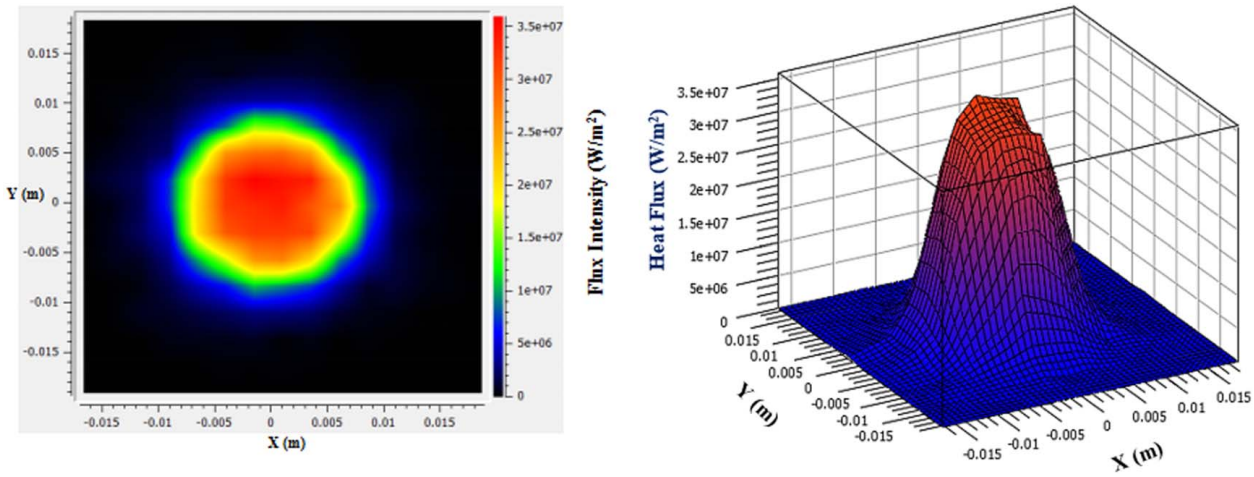

Fig. 5 Contour plot and surface plot of solar flux intensity at the concentrator's absorber for pillbox sun shape

4.2 SolTrace Result Validation. This validation was performed by comparing the numerical results obtained from SolTrace with a theoretical solar flux intensity analysis on the focal plane of dish concentrator by Jeter [42] and OptisWorks simulation of flux distribution on a cylindrical cavity receiver by Jian et al. [23].

A dish concentrator with an aperture diameter of 2.308 m and focal length of 1 m with a reflectivity of material 0.9 and a black body absorber surface was used for validation. The comparison was made for incident solar radiation of 1000 W/m^2, and the corresponding simulation parameters were the same as Jeter, as shown in Table 4. It could be noted that the sun shape, optical error, and diameter of the receiver are different from the literature. The flux distribution was determined using a slope error of 0.35 mrad, a specularity error of 0.2 mrad, and a receiver diameter of 0.2 m. The solar irradiance distribution at the dish concentrator receiver obtained in this study for different sun shapes and the result reported by Jian et al. are presented in Fig. 6. The gaussian sun shape distribution has more consistency and peak flux than the pillbox sun shape. The deviation between the current study and literature can be attributed due to receiver geometry, optical error, and the number of rays intersection generated on the dish concentrator receiver. The slope error causes a deviation of radiation flux in the direction of the reflected receiver due to the surface error and tracking system. Table 5 depicts the result of heat flux distribution along with the radial position of the dish concentrator receiver of the current work for Pillbox and Gaussian distribution with a theoretical analysis by Jeter and Optiswork simulation result of Jian et al. The size of the absorber and slope error significantly impact the uniformity of heat flux distribution, receiver surface temperature, and

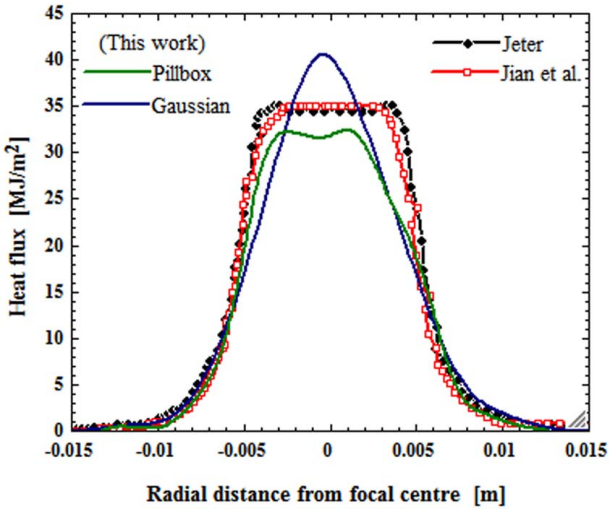

Fig. 6 Comparison of the solar irradiance distribution at different sun shapes (pillbox and gaussian) of the current study with the result reported by Jian et al. [23]

Table 4 Parameters of solar dish concentrator and receiver system

Parameter	Jeter [42]	Jian et al. [23]
Radius of dish concentrator (m)	1.154	7.0
Focal length of dish concentrator (m)	1.0	8.45
Reflectivity of concentrator surface	0.9	0.93
Absorptivity of plane receiver	1.0	0.95
Solar direct normal irradiance (W/m^2)	1000	800
Height of cavity receiver (mm)	–	350
Radius of the cavity receiver (mm)	–	140
Solar half-angle	Uniform sun shape	4.65 mrad
Slope error	–	–
Specularity error	–	–
Receiver type	–	Cavity

Table 5 Solar flux intensity at the receiver surface

			This work (MW/m^2)	
Radial position from focal Centre (m)	Jeter (MW/m^2)	Jian et al. (MW/m^2)	Pillbox sun shape	Gaussian sun shape
−0.0115	0	0	0	0
−0.00967	1.975	1.03	0.3655	0
−0.00783	4.359	3.59	0.6091	0.05995
−0.00599	12.05	12.6	3.776	0.5995
−0.00415	33.08	31.3	11.7	1.978
−0.00231	34.72	34.9	28.38	10.37
−0.000476	34.62	35.1	32.16	27.04
0.00136	34.62	35.1	31.67	40.35
0.0032	35.13	34.4	31.92	32.91
0.00504	24.1	24.4	25.1	18.17
0.00688	6.667	6.41	17.3	5.875
0.00871	2.821	2.05	5.604	1.739
0.0106	1.282	0.769	1.827	0.2398
0.0124	0.7692	0.769	0.6091	0
0.0142	0.5128	0.513	0	0
0.0115	0	0.513	0	0

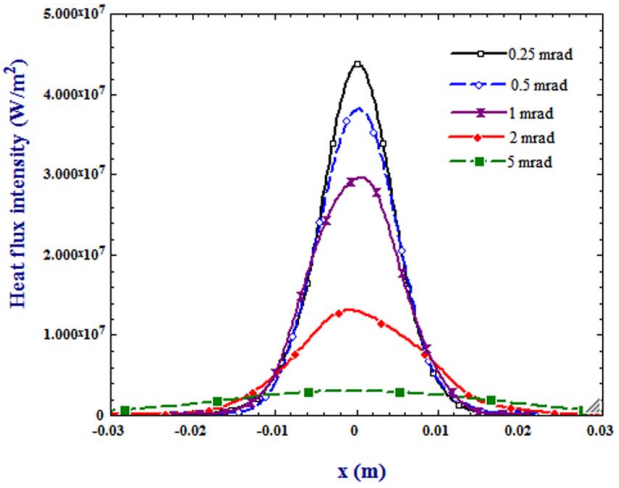

Fig. 7 Solar irradiance distribution profiles, varying slope error (0.25 mrad, 0.5 mrad, 1 mrad, 2 mrad, and 5 mrad)

optical performance of the concentrator. In consideration of these factors and assumptions employed by Jeter, including non-consideration of slope and specularity errors, it can be seen that the simulation results of pillbox sun shape agree well with the literature.

Solar heat flux distribution will be influenced by slope and specularity errors. The variation of slope error significantly impacts the uniformity of flux intensity and peak flux at the center of the absorber, as shown in Fig. 7. At low slope error, the peak flux at the focal plane of the concentrator is high, whereas, at high slope error, the peak flux and uniformity of the heat flux slightly decrease. It is because the rays reflected from the concentrator are no longer specularly reflected, and rays reach the surface of the absorber randomly distributed, and other rays will miss the absorber.

On the other hand, the effect of specularity error, as shown in Fig. 8, depicts relatively small changes in heat flux distribution. Increasing specularity error at a given value of slope error could cause a slight deviation in peak flux uniformity of solar irradiance distribution. At the different combinations of slope errors and specularity errors, the heat flux distribution on the dish concentrator receiver is non-uniform, and high heat flux is found at lower values of slope errors.

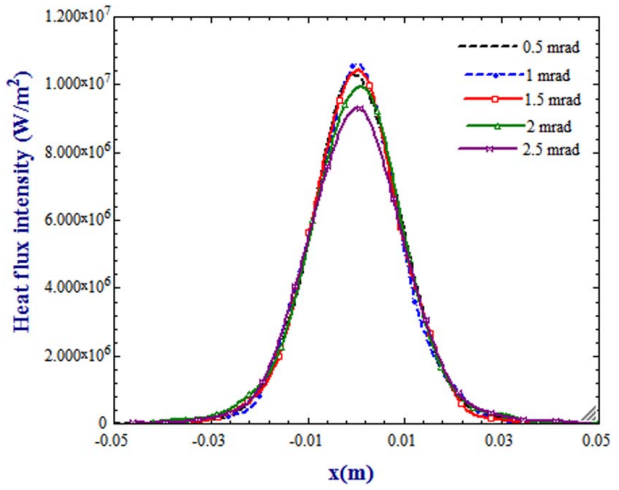

Fig. 8 Solar flux distribution at a focal plane of dish concentrator, varying specularity error from 0.5 to 2.5 mrad with increments of 0.5 mrad

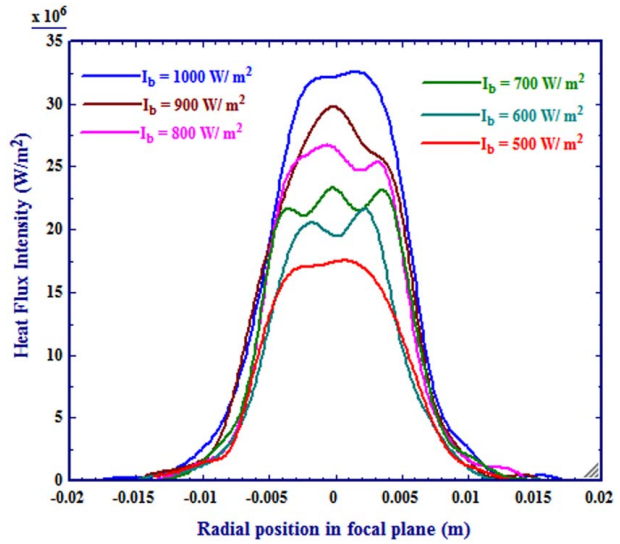

Fig. 9 Variation of heat flux distribution with beam solar radiation for pillbox sun shape

4.3 Effect of Beam Solar Radiation on Heat Flux. The heat flux intensity reaching the concentrator's absorber/receiver is affected by the variation of incoming solar radiation. For the same optical properties and receiver geometry, varying DNI from 500 to 1000 W/m^2 with an increment of 100 W/m^2 increases the heat flux intensity from 17.5 to 32.4 MW/m^2. The flux distribution on the focal plane increases toward the center with increasing solar irradiation, as shown in Fig. 9. Depending on the material properties and size of the receiver, high direct normal irradiance increased heat flux intensity. Varying DNI influences power plotted per rays. Increasing DNI value increases peak flux and power plotted per rays in the radial position from the periphery to the center of the absorber.

4.4 Effect of Solar Heat Flux on Temperature Distribution. The temperature distribution analysis at the dish concentrator receiver was done through COMSOL MULTIPHYSICS V5.5 [43]. The simulation was carried out using the heat transfer module

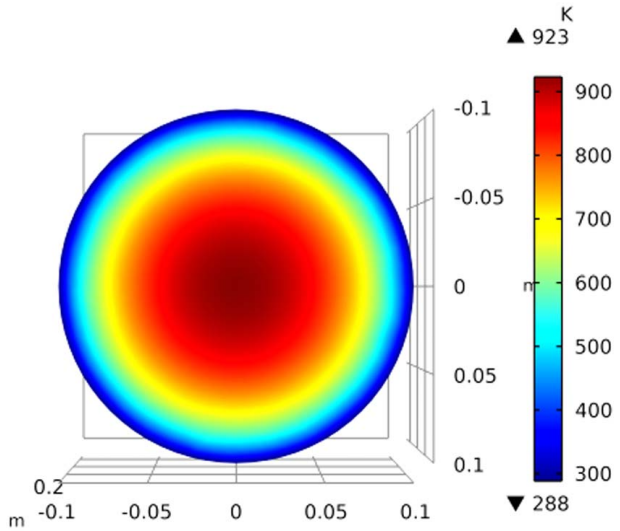

Fig. 10 Temperature distribution at the receiver of the concentrator

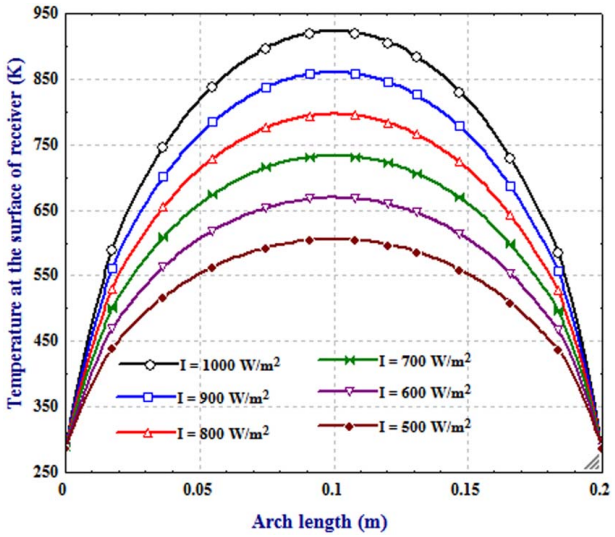

Fig. 11 Effect of beam solar radiation variation on temperature distribution at the surface of the receiver

package in the software. As boundary conditions, the solar flux intensity and ambient temperature of 298.12 K are employed, and the heat loss from the surface of the absorber was neglected. As shown in Fig. 10, the temperature distribution slightly decreases along with the radial position from the center to the absorber's edge. The result depicts that for the average heat flux of 4.75 MW/m^2, the receiver's surface temperature reaches 923 K at the center. The homogeneity of the flux distribution affects the uniformity of the temperature distribution. Non-uniform temperature distribution at the focal plane of the concentrator will be affected by heat transfer and heat loss, which in turn reduces thermal performance.

Figure 11 shows the impact of solar irradiance variation on the absorber focal plane's temperature distribution. Higher solar irradiance leads to higher temperatures being attained at the receiver focal plane. By varying the beam solar radiation from 500 to 1000 W/m^2, the receiver's center's temperature increases from 606 to 923 K. The thermal efficiency of the dish concentrator depends on the mass flowrate of the working fluid, temperature gradient, direct normal irradiance, aperture area, and optical efficiency. For a given mass flowrate and aperture area, increasing DNI will increase the resultant temperature and losses from the absorber of the concentrator. At a specific DNI value and low optical error, increasing the receiver surface temperature by shape optimization could increase the concentrator's optical and thermal efficiency, which can have a cascading effect at higher values of DNI.

5 Conclusion

This work focused on analyzing heat flux intensity distribution and its effect on resultant temperature distribution at the focal plane of the solar dish concentrator. The optical performance of the dish concentrator can be enhanced by reducing the optical error and heat losses from the absorber. The optical error should be minimized by determining the heat flux intensity reaching the surface of the receiver and analyzing the temperature distribution at the focal plane of the concentrator. The slope and specularity error reduces the uniformity of heat flux and thus the temperature distribution as well, which in turn influences the optical and thermal performance of the concentrator. The amount of heat flux depends on the absorber's cross-sectional area and the amount of solar irradiance it receives. The heat flux and temperature distribution are higher in the absorber's middle portion and diminish as it moves outward. Higher beam solar radiation leads to higher heat flux and temperature distribution to achieve higher useful thermal heat. In this work, the analysis was carried out using a cylindrical receiver where the peak heat flux and temperatures attained are 32.4 MW/m^2 and 923 K, respectively. Still, more research needs to be carried out with other absorber types to determine the optimum performance. The impact of the intercept factor on receiver performance also needs to be examined.

Conflict of Interest

There are no conflicts of interest. All procedures performed for studies involving human participants were in accordance with the ethical standards stated in the 1964 Declaration of Helsinki and its later amendments or comparable ethical standards? Informed consent was obtained from all participants. Documentation provided upon request. Informed consent is not applicable. This article does not include any research in which animal participants were involved.

Data Availability Statement

The data sets generated and supporting the findings of this article are obtainable from the corresponding author upon reasonable request. The authors attest that all data for this study are included in the paper. Data provided by a third party are listed in Acknowledgment. No data, models, or code were generated or used for this paper.

References

[1] Hafez, A. Z., Soliman, A., El-Metwally, K. A., and Ismail, I. M., 2017, "Design Analysis Factors and Specifications of Solar Dish Technologies for Different Systems and Applications," Renewable Sustainable Energy Rev., **67**, pp. 1019–1036.

[2] Mao, Q., Shuai, Y., and Yuan, Y., 2014, "Study on Radiation Flux of the Receiver With a Parabolic Solar Concentrator System," Energy Convers. Manage., **84**, pp. 1–6.

[3] Senthil, R., and Cheralathan, M., 2017, "Effect of Non-uniform Temperature Distribution on Surface Absorption Receiver in Parabolic Dish Solar Concentrator," Therm. Sci., **21**(5), pp. 2011–2019.

[4] Nyeinga, K., Okello, D., and Nydal, O. J., 2019, "A Ray Tracer Model for Analysis of Solar Concentrating Systems," J. Energy South. Afr., **30**(1), pp. 8–20.

[5] Zhang, G., Wei, J., Zhang, L., Xi, C., Ding, R., Wang, Z., and Khalid, M., 2021, "A Comprehensive Study on the Effects of Truncation Positions of the Compound Parabolic Concentrator Eliminating Multiple Reflections on the Performances of Concentrating Photovoltaic and Thermal Systems," Appl. Therm. Eng., **183**, p. 116162.

[6] Zhang, G., Wei, J., Xie, H., Wang, Z., Xi, Y., and Khalid, M., 2018, "Performance Investigation on a Novel Spectral Splitting Concentrating Photovoltaic/Thermal System Based on Direct Absorption Collection," Sol. Energy, **163**(10), pp. 552–563.

[7] Pavlovic, S. R., Stefanović, V. P., Rajković, P., Petrovic, E. P., and Ayed, S., 2015, "Ray Tracing Study to Determine the Characteristics of the Solar Image in the Receiver for a Thermal Solar Concentration System," Proceeding of the 7th International Symposium on Exploitation of Renewable Energy Sources and Efficiency, EXPRESS, Subotica, Serbia, Mar. 19–21, pp. 35–39.

[8] Zhang, W. W., Qi, H., Ji, Y. K., He, M. J., Ren, Y. T., and Li, Y., 2021, "Boosting Photoelectric Performance of Thin-Film GaAs Solar Cell Based on Multi-objective Optimization for Solar Energy Utilization," Sol. Energy, **230**(6), pp. 1122–1132.

[9] Nie, D. Z., Peng, Y. D., Yan, J., Mi, C. J., Liu, Y. X., and Tian, Y., 2020, "Improvement in the Flux Uniformity of the Solar Dish Concentrator System Through a Concave Quartz Window," Int. J. Photoenergy, pp. 1–16.

[10] Fontani, D., Sansoni, P., Francini, F., Toni, F., and Jafrancesco, D., 2022, "Optical Raytracing Analysis of a Scheffler Type Concentrator," Energies, **15**(1), p. 260.

[11] Santos, A. V., Canavarro, D., Horta, P., and Collares-Pereira, M., 2021, "An Analytical Method for the Optical Analysis of Linear Fresnel Reflectors With a Flat Receiver," Sol. Energy, **227**(5), pp. 203–216.

[12] Cisneros-Cárdenas, N. A., Cabanillas-López, R., Pérez-Enciso, R., Martínez-Rodríguez, G., García-Gutiérrez, R., Pérez-Rábago, C., Calleja-Valdez, R., and Riveros-Rosas, D., 2021, "Study of the Radiation Flux Distribution in a Parabolic Dish Concentrator," Energies, **14**(21), p. 7053.

[13] Yan, J., Cheng, Z. R., and Peng, Y. D., 2018, "Effects of Geometrical Parameters of a Dish Concentrator on the Optical Performance of a Cavity Receiver in a Solar Dish-Stirling System," Int. J. Energy Res., **42**(6), pp. 2152–2168.

[14] Bopche, S., Rana, K., and Kumar, V., 2020, "Performance Improvement of a Modified Cavity Receiver for Parabolic Dish Concentrator at Medium and High Heat Concentration," Sol. Energy, **209**, pp. 57–78.
[15] Jae Lee, B., Chen, Y. B., Han, S., Chiu, F. C., and Jin Lee, H., 2014, "Wavelength-Selective Solar Thermal Absorber With Two-Dimensional Nickel Gratings," ASME J. Heat Transfer-Trans. ASME, **136**(7), p. 072702.
[16] Yang, D., Zhao, X., Liu, Y., Li, J., Liu, H., Hu, X., Li, Z., et al.et al., 2020, "Enhanced Thermal Stability of Solar Selective Absorber Based on Nano-multilayered AlCrSiO Films," Sol. Energy Mater. Sol. Cells, **207**(9), p. 110331.
[17] Zhang, W. W., Qi, H., Yu, Z. Q., He, M. J., Ren, Y. T., and Li, Y., 2021, "Optimization Configuration of Selective Solar Absorber Using Multi-island Genetic Algorithm," Sol. Energy, **224**(6), pp. 947–955.
[18] Mwesigye, A., Bello-Ochende, T., and Meyer, J. P., 2014, "Minimum Entropy Generation due to Heat Transfer and Fluid Friction in a Parabolic Trough Receiver with Non-uniform Heat Flux at Different Rim Angles and Concentration Ratios," Energy, **73**(1), pp. 606–617.
[19] Zhao, D., Xu, E., Yu, Q., and Lei, D., 2015, "The Simulation Model of Flux Density Distribution on an Absorber Tube," Energy Procedia, **69**, pp. 250–258.
[20] Mwesigye, A., Bello-Ochende, T., and Meyer, J. P., 2015, "Numerical Investigation of the Effect of Slope Errors and Specularity Errors on the Thermal Performance of a Solar Parabolic Trough Collector System," Proceedings of the SASEC2015 Third Southern African Solar Energy Conference, Kruger National Park, South Africa, May 11–13, pp. 88–93.
[21] Wang, Y., Potter, D., Asselineau, C. A., Corsi, C., Wagner, M., Caliot, C., Piaud, B., Blanco, M., Kim, J. S., and Pye, J., 2020, "Verification of Optical Modelling of Sunshape and Surface Slope Error for Concentrating Solar Power Systems," Sol. Energy, **195**(7), pp. 461–474.
[22] Butti, L., Manuel, J., Tripp, N. G., Núñez Mc Leod, J. E., and Rivera, S. S., 2021, "Effect of Surface Material Properties and Operating Conditions on the Heat Flux and Temperature Distributions in the Cavity Receiver of a Solar-Dish-Coupled Biomass Gasification Reactor," Energy Convers. Manage., **244**, p. 114303.
[23] Yan, J., Peng, Y. D., and Cheng, Z. R., 2018, "Mirror Rearrangement Optimization for Uniform Flux Distribution on the Cavity Receiver of Solar Parabolic Dish Concentrator System," Int. J. Energy Res., **42**(11), pp. 3588–3614.
[24] Kopalakrishnaswami, A. S., and Natarajan, S. K., 2022, "Comparative Study of Modified Conical Cavity Receiver With Other Receivers for Solar Paraboloidal Dish Collector System," Environ. Sci. Pollut. Res., **29**(5), pp. 7548–7558.
[25] Mao, Q., Zhang, L., and Wu, H., 2015, "Study on Concentrating Characteristics of a Solar Parabolic Dish Concentrator Within High Radiation Flux," Int. J. Photoenergy, pp. 1–7.
[26] Bellos, E., Bousi, E., Tzivanidis, C., and Pavlovic, S., 2019, "Optical and Thermal Analysis of Different Cavity Receiver Designs for Solar Dish Concentrators," Energy Convers. Manage.: X, **2**(6), p. 100013.
[27] Missana, W. P., Park, E., and Kivevele, T. T., 2020, "Thermal Performance Analysis of Solar Dryer Integrated With Heat Energy Storage System and a Low-Cost Parabolic Solar Dish Concentrator for Food Preservation," J. Energy, pp. 1–10.
[28] Craig, O. O., 2015, *A Stand-Alone Parabolic Dish Solar Cooker for African Conditions*, Stellenbosch University, Stellenbosch.
[29] Wang, L., Yuan, Z., Zhao, Y., and Guo, Z., 2019, "Review on Development of Small Point-Focusing Solar Concentrators," J. Therm. Sci., **28**(5), pp. 929–947.
[30] Chong, K.-K., and Wong, C.-W., 2010, "General Formula for On-Axis Sun-Tracking System," Sol. Collect. Panels, Theory Appl., **444**, pp. 264–292.
[31] Thakkar, V., Doshi, A., and Rana, A., 2015, "Performance Analysis Methodology for Parabolic Dish Solar Concentrators for Process Heating Using Thermic Fluid," J. Mech. Civ. Eng., **12**(1), pp. 101–114.
[32] Stine, W. B., and Diver, R. B., 1994, "A Compendium of Solar Dish/Stirling Technology, SAND93-7026 UC-236," http://www.osti.gov/energycitations/servlets/purl/10130410-xiVU1 V/native/%5Cn10.2172/10130410.
[33] Kalogirou, S. A., 2004, "Solar Thermal Collectors and Applications," Prog. Energy Combust. Sci., **30**(3), pp. 231–295.
[34] Skouri, S., Bouadila, S., and Nassrallah, S. B., 2016, "Improvement of Solar Parabolic Concentrator Thermal Efficiency Correlated to Different Factors," IOSR J. Mech. Civ. Eng., **16**(053), pp. 67–73.
[35] Nassrallah, S. B., 2016, "Improvement of Solar Parabolic Concentrator Thermal Efficiency Correlated to Different Factors," IOSR J. Mech. Civ. Eng., **16**(053), pp. 67–73.
[36] Hafez, A. Z., Soliman, A., El-Metwally, K. A., and Ismail, I. M., 2016, "Solar Parabolic Dish Stirling Engine System Design, Simulation, and Thermal Analysis," Energy Convers. Manage., **126**, pp. 60–75.
[37] Kalogirou, S., 2009, "Solar Energy Engineering," J. Sol. Energy Eng., **116**(2), pp. 67–68.
[38] Cherif, H., Ghomrassi, A., Sghaier, J., Mhiri, H., and Bournot, P., 2019, "A Receiver Geometrical Details Effect on a Solar Parabolic Dish Collector Performance," Energy Rep., **5**, pp. 882–897.
[39] Wendelin, T., 2003, "SolTrace: A New Optical Modeling Tool for Concentrating Solar Optics," Proceedings of the International Solar Energy Conference, Kohala Coast, HI, Mar. 15–18, pp. 253–260.
[40] Wendelin, T., Dobos, A., and Lewandowski, A., 2013, *SolTrace: A Ray-Tracing Code for Complex Solar Optical Systems*, National Renewable Energy Lab. (NREL), Golden, CO.
[41] Yang, S., Wang, J., Lund, P. D., Jiang, C., and Liu, D., 2018, "Assessing the Impact of Optical Errors in a Novel 2-Stage Dish Concentrator Using Monte-Carlo Ray-Tracing Simulation," Renewable Energy, **123**, pp. 603–615.
[42] Jeter, S. M., 1986, "The Distribution of Concentrated Solar Radiation in Paraboloidal Collectors," ASME J. Sol. Energy Eng., **108**(3), pp. 219–225.
[43] COMSOL, 2018, "COMSOL Multiphysics® v. 5.5," 1742.